ACS Sustainable Resource Management

pubs.acs.org/acssrm

Article

High-Sulfur-Content Materials Derived from Postconsumer Polystyrene Wastes: Thermomechanical Properties, Environmental Impacts, and Microstructural Insights

Shalini K. Wijeyatunga, Andrew G. Tennyson,* and Rhett C. Smith*

Cite This: https://doi.org/10.1021/acssusresmgt.4c00085

Read Online

ACCESS | Metrics & More | Article Recommendations | Supporting Information

ABSTRACT: Postconsumer polystyrene (PS) wastes are a major contributor to microplastic contamination of the biosphere, which could be reduced or eliminated by developing strategies to upcycle these wastes into useful materials. Four postconsumer PS waste streams from flatware (**PSF**), cups (**PSC**), lids (**PSL**), and packaging materials (**PSP**), as well as a mixture of all four streams (**PSM**), were reacted with elemental sulfur at 230 °C to afford the corresponding high-sulfur-content materials (HSMs) **PSF$_{90}$**, **PSC$_{90}$**, **PSL$_{90}$**, **PSP$_{90}$**, and **PSM$_{90}$**, respectively. Glass transitions in these HSMs were observed at temperatures ranging from −36 to −39 °C, with these values being characteristic of oligo/polysulfide chains. Compressional and flexural strength measurements revealed that these HSMs were competitive with ordinary Portland cement and C62 Brick. To gain insight into the microstructural features within these HSMs, cumene was reacted with sulfur at 230 °C and then depolymerized with $LiAlH_4$, yielding small-molecule products amenable to GC-MS analysis. These reactivity studies provided compelling evidence that **PSF$_{90}$**, **PSC$_{90}$**, **PSL$_{90}$**, **PSP$_{90}$**, and **PSM$_{90}$** contain the expected oligo/polysulfide cross-links between PS chains at 3° benzylic and 2° aliphatic carbons in addition to the formation of benzothiophene moieties.

KEYWORDS: *Polystyrene, Sulfur Utilization, Upcycling, Thiocracking, Composites*

INTRODUCTION

Global plastic production exceeds 450 Mt each year, with more than 150 Mt of polypropylene, 60 Mt of polyethylene, 30 Mt of poly(ethylene terephthalate), and 25 Mt of polystyrene, with most of this mass found in single-use consumer products.[1] Each of these polymers exhibits thermoplastic behavior, but industrial-scale melt-recycling is practical for only polypropylene, polyethylene, and poly(ethylene terephthalate) with current technology. Recycling polystyrene (PS) is complicated by the fact that it is commonly blended with other materials, some of which are incompatible with melt-recycling processes.[2] Because the largest application of PS is disposable packaging and food service items, a significant proportion of postconsumer PS is discarded in mixed-waste streams. Unfortunately, postconsumer PS wastes are highly dispersible and thus contribute significantly to microplastic contamination of both terrestrial[3] and marine[4] environments.

Despite the obvious environmental harms of PS wastes, <1% of nondurable PS-based products—such as plastic flatware, single-use cups and lids, and packaging—are not recycled due to the aforementioned challenges. To prevent postconsumer PS wastes from entering the biosphere and causing grave environmental damage, there is an urgent need to develop new strategies to recycle postconsumer PS wastes or upcycle them into useful materials via processes that can be economically viable and technically feasible on industrial scales. Significant progress has recently been made in upcycling by depolymerizing PS into (i) small-molecule aromatic building blocks for chemical synthesis using photocatalytic oxidation,[5−10] thermal oxidation,[11−15] and mechanochemical force,[16] (ii) transportation fuel-grade hydrocarbons using microwave,[17,18] and (iii) biocidal natural products using bioengineered enzymes,[19] as well as by incorporating PS into versatile composites suitable for use in applications ranging from catalysis[20] to electrophoretic imaging[21] to CO_2 sequestration.[22]

Petroleum refining produces significant quantities of elemental sulfur from hydrodesulfurization processes, but because sulfur production outpaces productive applications, large quantities of it enter the biosphere at open-air, outdoor waste storage sites. Given the magnitude of annual sulfur waste

Received: March 5, 2024
Revised: September 13, 2024
Accepted: September 13, 2024

Scheme 1. HSM Formation[a]

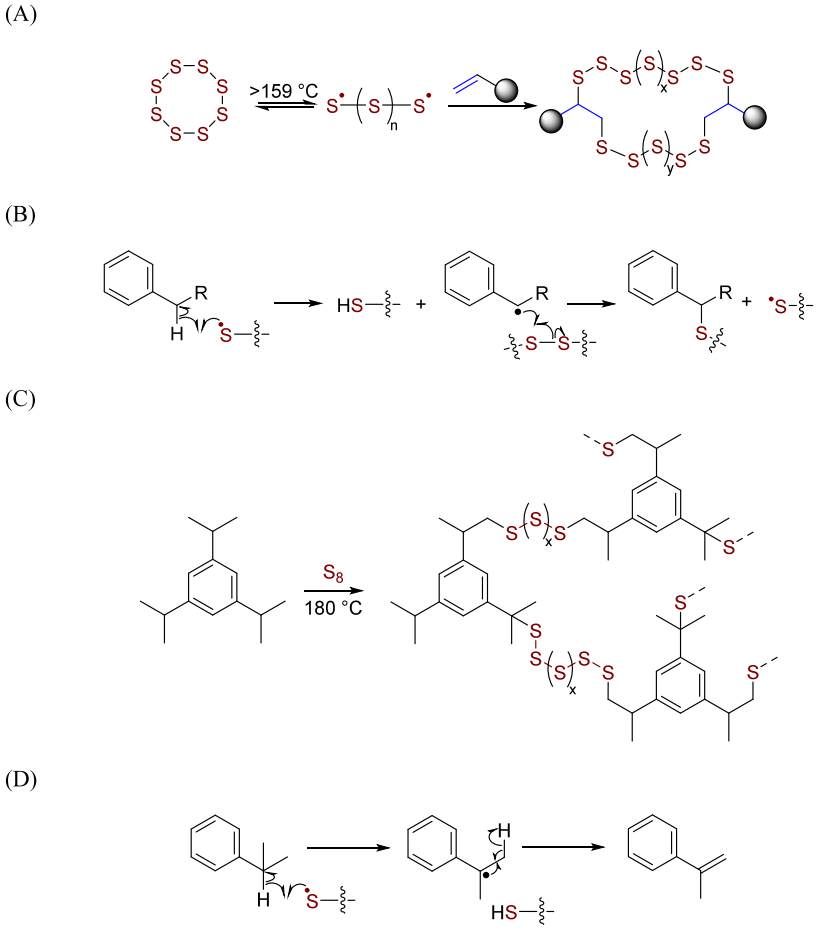

[a]Sulfur−carbon bond formation can be accomplished by inverse vulcanization of alkenes (A) and S−$C_{benzylic}$ bond formation (B). Even in the absence of alkenes, S−$C_{benzylic}$ bond formation can support the formation of composites, as demonstrated by reactions of 1,3,5-triisopropylbenzene with S_8 at 180 °C (C). Alkenes can be formed from benzylic alkyl groups as shown in (D).

production (82 Mt),[23] the sulfur at these storage sites poses hazards to waste-management personnel[24] and can cause acidification of the nearby soil and groundwater.[25−27] As a result, better sulfur utilization is an area actively explored to support sustainability and environmental remediation goals, ranging from optical sensors to thermosets.[28−35] Inverse vulcanization (InV)[36,37] has emerged as a revolutionary process to upcycle sulfur into valuable products, which will reduce the amount of new sulfur waste entering the environment and, eventually, begin to consume the vast stockpiles of existing sulfur waste. The mechanism underlying the InV reaction is the addition of oligo/polymeric sulfide radicals, thermally generated via ring-opening of S_8, to C=C π-bonds, affording new C−S σ-bonds. InV reactions are often performed with a mass of alkene substrate smaller than that of S_8;[38−50] thus, the products of InV reactions are often described as high-sulfur-content materials (HSMs). A common feature of HSMs is the presence of cross-linking oligo/polysulfide chains between organic substrates that are anchored by C−S σ-bonds.

Pyun and co-workers have demonstrated that styrene monomer can react with S_8 to produce HSMs comprised of oligo/polysulfide cross-links between the styrene monomers (Scheme 1A−1B), concomitant with formation of poly/oligostyrene chains.[51,52] The predominant microstructural features are linear chains comprised of alternating oligo/polysulfide and styrene subunits, which are produced via addition of sulfur-centered radicals to C=C π-bonds. Alternatively, HSMs can also be generated upon reaction of S_8 with organic substrates that contain no olefinic groups. For example, Lai and Liu demonstrated that 1,3,5-triisopropylbenzene (TIPB) could react with S_8 to afford an HSM product, which interestingly contained cross-linking oligo/polysulfide chains tethered to TIPB cores, consistent with the addition of sulfur radicals to olefinic groups (Scheme 1C−1D).[53] The authors proposed that the reaction conditions caused H atom abstraction followed by elimination, which generated olefinic groups in situ. To reflect the distinction between the reaction pathways initiated by olefin addition from those initiated by H atom transfer (HAT), we will describe the former as "olefin-addition-initiated S−C bond-forming reactions" (i.e., traditional InV) and the latter as "HAT-initiated S−C bond-forming reactions."

Because polystyrene contains tertiary benzylic sites similar to those in TIPB, we hypothesized that PS itself would react with S_8 to form S−C bonds at the (i) 3° benzylic sites, via H atom abstraction to form 3° benzylic radicals, as well as the (ii) 2° aliphatic sites, via in situ generation of olefinic moieties from 3° benzylic radicals, to afford HSMs comprised of polymeric carbon chains cross-linked by oligo/polysulfide branches. Four postconsumer PS waste streams were selected as the organic

https://doi.org/10.1021/acssusresmgt.4c00085
ACS Sustainable Resour. Manage. XXXX, XXX, XXX−XXX

inputs for reaction with S_8 based on their prevalence: flatware, foam cups, lids (those that fit the foam cups that were used), and shipping packaging cubes. Herein we report the reactions of S_8 at 230 °C with each of these PS waste streams, as well as with mixed samples containing all four PS wastes, to give composites **PSF$_{90}$**, **PSC$_{90}$**, **PSL$_{90}$**, **PSP$_{90}$**, and **PSM$_{90}$**, respectively (using the abbreviation **PSX$_{yy}$**, where **PS** refers to polystyrene, **X** refers to the specific waste stream source, and ***yy*** refers to the mass % of S_8 in the HSM product). The results from spectroscopic, thermomechanical, mass spectrometric, and sustainability analyses of these HSMs are presented and compared to representative construction materials.

RESULTS AND DISCUSSION

Preparation and Characterization of Postconsumer Polystyrene Waste Samples. Four high-volume sources of postconsumer polystyrene (PS) wastes were selected for testing in the current study: (1) PS flatware (**PSF**) recovered from office refuse, (2) PS foam cups (**PSC**) recovered from fast food restaurant refuse, (3) the PS lids associated with those cups (**PSL**), and (4) PS packaging cubes (**PSP**) recovered from shipping boxes (Figure 1). Samples of **PSF**, **PSC**, **PSL**, and **PSP** were ground in an industrial blender to yield free-flowing particulate materials suitable for use in thiocracking reactions. To reflect the heterogeneous nature of postconsumer plastic wastes, mixed PS samples (**PSM**) were prepared using input streams containing **PSF**, **PSC**, **PSL**, and **PSP**. For this purpose, it was reasoned that the cup- and lid-derived polystyrene would generally be disposed of as a unit (3:1 ratio of **PSC**:**PSL** by mass). The polystyrene waste was then mixed in a 1:1:1 ratio (**PSP**:**PSC**/**PSL**:**PSF**) to make up the mixed **PSM** feedstock.

Figure 1. Samples of postconsumer polystyrene used for this study showing the items as-collected (left column), during grinding (middle column), and after grinding (right column). Grey shapes have been added to the as-collected images of the cup and lid to cover trademarked images of the restaurant chain from which the refuse samples were collected.

Infrared spectroscopic analysis of **PSF**, **PSC**, and **PSP** samples revealed spectra that were highly conserved across the series (Figures S1–S3) and in good agreement with IR spectra for pure PS (Figure S4). Samples of **PSL** displayed additional peaks in the 950–1000 cm^{-1} region attributable to polybutadiene added to improve the toughness of PS to be suitable for cup lids (Figure S5). Proton NMR spectra of **PSF**, **PSC**, and **PSP** samples (Figures S6–S8) were likewise consistent with the ^{1}H NMR spectra of pure PS (Figure S9). The ^{1}H NMR spectrum of **PSL** was similar to those of **PSF**, **PSC**, and **PSP** samples but also included signals unique to **PSL**, most notably a resonance at 5.39 ppm, which indicated the presence of alkene protons (Figure S10). The type of polystyrene most commonly used in disposable drink container lids is high-impact polystyrene (HIPS),[54] which is a composite of polystyrene blended with a polybutadiene additive to enhance its toughness and flexibility. Because the polybutadiene content in HIPS typically ranges from 3 to 10 wt %,[55,56] we therefore attributed the signal at 5.39 ppm in the ^{1}H NMR spectrum of **PSL** to the polybutadiene additive present in that material.

Molecular-weight analyses of **PSF**, **PSC**, **PSL**, and **PSP** by gel-permeation chromatography (GPC) yielded number-averaged molecular weight (M_n) and dispersity ($Đ$) values within the ranges of 70–95 kDa and 1.6–1.9, respectively (Figures S11–S14 and Table S1). The GPC trace collected for **PSL** contained an additional small peak with M_n = 1100 Da that likely derives from the polybutadiene additive. Thermogravimetric analysis (TGA) of **PSF**, **PSC**, **PSL**, and **PSP** revealed decomposition temperatures (defined as the temperature at which 5% mass loss was observed, abbreviated as $T_{d,5\%}$) that were highly conserved across the series (371–388 °C) and similar to the values observed with pure PS (Figures S15–S18). Broad glass transitions were observed in the differential scanning calorimetry (DSC) thermograms of these four PS waste stream samples, with their $T_{g,DSC}$ values ranging from 95 to 103 °C (Figures S19–S22), consistent with previously reported values for pure polystyrene.

Preparation and Characterization of HSMs from Postconsumer Polystyrene Wastes. Initial attempts at inverse vulcanization of **PSF**, **PSC**, **PSL**, and **PSP** were performed at 180 °C, given that H atom abstraction and S–$C_{benzylic}$ bond formation occur at this temperature when the substrate is 1,3,5-triisopropylbenzene (Scheme 1C). However, using these conditions with **PSF**, **PSC**, **PSL**, and **PSP** afforded highly heterogeneous materials in which macroscopic pieces of unreacted PS were still present, even after 24 h. Increasing the reaction temperature to 230 °C caused each of these PS samples to soften and homogenize with the molten sulfur. Reactions of **PSF**, **PSC**, **PSL**, **PSP**, and **PSM** with sulfur at 230 °C afforded the corresponding HSMs **PSF$_{90}$**, **PSC$_{90}$**, **PSL$_{90}$**, **PSP$_{90}$**, and **PSM$_{90}$** as macroscopically homogenous black solids with no apparent unreacted PS particulates. Negligible mass loss due to H_2S(g) release (<0.33 wt %, Table S1) was observed during the syntheses of these HSMs. Scanning electron microscopy with elemental mapping by energy dispersive X-ray analysis (SEM–EDX) further demonstrated that each HSM was microscopically homogenous containing uniform elemental distributions of carbon and sulfur (Figure S23).

Sulfur atoms in HSMs can exist in either (a) oligo/polysulfide chains covalently tethered to organic species via C–S bonds, (b) crystalline sulfur noncovalently incorporated into the HSM network, or (c) amorphous oligo/polymeric sulfur species containing no C–S bonds that are instead merely physically entrapped in the HSM network. Whereas covalently tethered oligo/polysulfide chains and crystalline sulfur can be detected using DSC, amorphous oligo/polymeric sulfur species cannot. These amorphous sulfur species also cannot be

https://doi.org/10.1021/acssusresmgt.4c00085
ACS Sustainable Resour. Manage. XXXX, XXX, XXX–XXX

detected by IR or NMR spectroscopy; thus, they are classified as "dark sulfur" species, and, despite containing no covalent bonds to the HSM network, they can significantly impact the thermomechanical properties of the HSMs that contain them.[57,58] Fortunately, the dark sulfur content in an HSM can be quantified using UV−visible spectroscopy, whereby the dark sulfur present in an HSM is extracted out using an organic solvent, and its concentration in the extract can be measured using the absorbance at 275 nm.[58] With known values for the dark sulfur concentration and volume of the extract, the mass of dark sulfur removed from each HSM could be calculated. The relative wt % of dark sulfur in each HSM was obtained by dividing the mass of dark sulfur removed by the initial mass of the HSM. Performing these analyses on **PSF_{90}**, **PSC_{90}**, **PSL_{90}**, and **PSP_{90}** revealed relative dark sulfur contents ranging from 23 to 54 wt % (Table 1), values consistent with other HSMs

Table 1. Thermal and Morphological Properties of the Polystyrene−Sulfur Composites PSF_{90}, PSC_{90}, PSL_{90}, and PSP_{90} and Compared to S_8

materials	T_d[a] (°C)	T_m[b] (°C)	$T_{g,DSC}$[c] (°C)	dark sulfur (wt %)[d]
PSF_{90}	217	113	−36	23
PSC_{90}	226	118	−39	54
PSL_{90}	217	117	−39	40
PSP_{90}	220	118	−39	42
S_8	229	118	NA	NA

[a]The temperature at which the 5% mass loss was observed. [b]The temperature at the peak maximum of the endothermic melting. [c]Glass transition temperature. [d]Percent ethyl acetate-extractable sulfur species.

prepared by our group that incorporate postconsumer plastic wastes as the organic tethers for oligo/polysulfide chains.[59−61] Furthermore, other groups have reported dark sulfur content values approaching 20 wt % in HSMs prepared from both petroleum-derived and biosynthesized small-molecule olefins.[62−64] For the PS-derived HSMs reported in this work (**PSF_{90}**, **PSC_{90}**, **PSL_{90}**, and **PSP_{90}**), no statistically significant net increase or decrease in dark sulfur content was observed over the course of 8 days (Figure S24).

Thermal and Mechanical Properties of Composites. Thermogravimetric analyses of **PSF_{90}**, **PSC_{90}**, **PSL_{90}**, and **PSP_{90}** (Figures S25−S28) revealed a narrow distribution of $T_{d,5\%}$ values (217−226 °C) slightly below that of S_8 ($T_{d,5\%}$ = 229 °C, Table 1). The glass transition values from DSC analysis ($T_{g,DSC}$) of these HSMs ranged from −36 to −39 °C (Figures S29−S36) and were consistent with other HSMs reported by our group.[65,66] Glass transitions in this temperature range are characteristic of oligo/polymeric sulfur chains covalently anchored to nonsulfur atoms.[67,68] A narrow distribution of melting temperatures (T_m) for **PSF_{90}**, **PSC_{90}**, **PSL_{90}**, and **PSP_{90}** was also observed (T_m = 113−118 °C), the values and peak shapes of which were comparable to those for data from pure S_8 (118 °C). The $T_{d,5\%}$, $T_{g,DSC}$, and T_m values observed for **PSF_{90}**, **PSC_{90}**, **PSL_{90}**, and **PSP_{90}** were highly conserved with other previously reported HSMs.[59,69,70] Less than 0.1 wt % water absorption was measured for **PSC_{90}**, **PSL_{90}**, and **PSP_{90}**, consistent with the highly hydrophobic nature of S_8 and the majority of the HSM masses being sulfur.

Samples of **PSF_{90}**, **PSC_{90}**, **PSL_{90}**, **PSP_{90}**, and **PSM_{90}** suitable for compressional, flexural, and tensile strength measurements were prepared by remelting these HSMs and casting them into the appropriate molds (Figure S37). All the average ± standard deviation values presented in Table 2 were calculated based on

Table 2. Mechanical Properties of Postconsumer Polystyrene Waste-Derived HSMs (PSF_{90}, PSC_{90}, PSL_{90}, PSP_{90}, and PSM_{90}),[a] Other Plastic-Derived HSMs, and Conventional Building Materials

materials	compressional strength (MPa)	flexural strength/ modulus (MPa)	ultimate tensile strength at break (MPa)
PSF_{90}[b]	7.8 ± 0.6	4.40 ± 0.54/ 584±60.8	1.75 ± 0.12
PSC_{90}	7.7 ± 0.9	2.95 ± 0.22/ 380 ± 39.0	2.15 ± 0.27
PSL_{90}	12.8 ± 1.9	3.19 ± 0.33/ 459 ± 71.7	1.92 ± 0.29
PSP_{90}	9.8 ± 1.2	2.39 ± 0.14/ 341 ± 22.7	1.97 ± 0.19
PSM_{90}	9.6 ± 0.3	3.87 ± 0.22/ 467 ± 50.5	2.25 ± 0.61[b]
mPES[b]	26.9±0.6	7.7 ± 0.2/ 320 ± 5.1	0.21 ± 0.04[c]
PGMA-S[d]	17.5 ± 2.8	4.76 ± 0.7/642	3.88 ± 1.20[d]
SPC_{90}	12.8 ± 1.6	3.12 ± 0.53	ND
C62 Brick	8.6	ND	ND
Portland Cement	17.0	3.7/580	ND

[a]Average ± standard deviation values for **PSF_{90}**, **PSC_{90}**, **PSL_{90}**, **PSP_{90}**, and **PSM_{90}** were each calculated from four independent experiments. [b]Composite made from 90 wt % sulfur and 10 wt % esterified PET. [c]Composite made from 90 wt % sulfur and 10 wt % olefin-derivatized (Geraniol) PMMA. [d]Composite made from 90 wt % sulfur 10 wt % poly(bisphenol A carbonate).

the measurements from four independently prepared samples of each HSM. Comparisons of the compressive strength values across this series of HSMs are complicated by the fact that these values overlap when the standard deviations from replicate experiments are included (Figure S38A and Table 2). For example, **PSL_{90}** exhibited the greatest compressive strength value (12.8 ± 1.9 MPa) of the series, but the difference between this value and that of the HSM with the next-highest compressive strength, **PSP_{90}** (9.8 ± 1.2 MPa), was not statistically significant. The differences between the values for **PSP_{90}** vs **PSM_{90}**, **PSP_{90}** vs **PSC_{90}**, and **PSC_{90}** vs **PSF_{90}** were likewise not statistically significant. Therefore, whereas the greater compressive strength value of **PSL_{90}** compared to **PSC_{90}** and **PSF_{90}** could reflect a higher cross-link density in **PSL_{90}**, which in turn could be attributed to the polybutadiene additives present in the **PSL** samples, this argument is weakened by the statistically equivalent compressive strength of **PSP_{90}** vs **PSL_{90}**, despite the fact that the **PSP** samples contained no polybutadiene.

Flexural and tensile strength values measured for **PSF_{90}**, **PSC_{90}**, **PSL_{90}**, **PSP_{90}**, and **PSM_{90}** all fell within relatively narrow ranges (2.39−4.40 and 1.75−2.25 MPa, respectively, Figures S38B and S38C). Stress−strain plots for each HSM are provided in the Supporting Information (Figures S39−S53). These findings suggest that the specific compositions of the polystyrene waste streams do not meaningfully impact the HSM properties. The compressional, flexural, and tensile strengths of **PSF_{90}**, **PSC_{90}**, **PSL_{90}**, **PSP_{90}**, and **PSM_{90}** were consistent with previously mreported HSMs, including those derived from other plastic wastes.[71−80] Ordinary Portland Cement (OPC) exhibits a higher compressional strength (17

https://doi.org/10.1021/acssusresmgt.4c00085
ACS Sustainable Resour. Manage. XXXX, XXX, XXX−XXX

MPa) than PSF_{90}, PSC_{90}, PSL_{90}, PSP_{90}, and PSM_{90}, but the flexural strength of OPC (3.7 MPa) falls within the range of values observed for these HSMs. A commonly used building material rated for structural masonry applications is C62 Brick, which exhibits a compressional strength (8.6 MPa) that is comparable to the values measured for PSF_{90}, PSC_{90}, PSL_{90}, PSP_{90}, and PSM_{90}. Impressively, these HSMs derived from postconsumer polystyrene waste streams could serve as sustainable alternatives to conventional building materials.

Preliminary Environmental Impact Estimates. The preparation of PSF_{90}, PSC_{90}, PSL_{90}, PSP_{90}, and PSM_{90} employs only waste materials—postconsumer polystyrene and elemental sulfur—as their precursors. The synthetic procedure and recovery of useful product is also simple, comprised of (1) grinding the polystyrene waste, (2) heating/stirring the PS and sulfur together, and (3) pouring molten material directly into molds to form the desired shapes. Recovery of the product is quantitative with no mass loss, amounting to a 100% atom economy and an *E* factor[81] of zero. These metrics reflect the excellent mass balance of the process but do not account for energy expenditures required of the process. A more complete estimate of such factors is provided by the global-warming potential, an estimate of kilograms of CO_2 emitted per kilogram of useful material made (kg CO_2e/kg), constrained to a set of assumptions for the process. For the calculation of the global-warming potential of the PS–sulfur composites, we use the reported global-warming potential of PS (~3.0 kg CO_2e/kg)[82] and estimate the amount of energy needed to grind the PS to be 0.092 kg CO_2e/kg based on estimates of grinding energy for PET.[83−88] To estimate the amount of energy needed to heat the reaction mixture from 20 to 230 °C and to hold it at that temperature for 24 h, we use metrics for sulfur, which makes up 90 wt % of the mixture. The energy needed was calculated to be 0.025 kg CO_2e/kg on the basis of the heat capacity and heat of fusion of sulfur[89] over the range of 20−230 °C and assuming a 90% efficiency for heat retention during the 24 h holding period and an average carbon intensity of 0.50 kg CO_2e/kWh for the electricity source. We also assume that if the polystyrene was not used for this process, it would instead be incinerated (producing 3.4 kg CO_2e/kg PS incinerated). The calculation based on these assumptions is summarized in Table 3. On the basis of these assumptions, the overall process is slightly carbon negative. It is important to note that these calculations do not include transportation costs, but the global-warming potential for the composites is considerably lower than that of mineral cements, which generally have a global warming potential of ~1.0 kg CO_2e/kg based on material and energy costs similar to those used for the calculation for the composites.[90,91]

Table 3. Metrics Used in the Calculation of the Global-Warming Potential of Composites (PSF_{90}, PSC_{90}, PSL_{90}, PSP_{90}, or PSM_{90})

process	cost (+) or credit (−)?	value (kg CO_2e)
make PS (0.10 kg × 3.0 kg CO_2e/kg)	+	0.30
grinding (0.100 kg of PS × 0.092 kg CO_2e/kg)	+	0.0092
heating (1.00 kg mixture × 0.025 kg CO_2e/kg)	+	0.025
prevent incineration of PS (0.100 kg × 3.4 kg CO_2e/kg)	−	0.34
	total	−0.0058 kg CO_2e/kg

Microstructural Insight from Model Studies. The highly cross-linked natures and insolubilities of PSF_{90}, PSC_{90}, PSP_{90}, PSL_{90}, and PSM_{90} precluded solution-phase analytical methods, hindering efforts to elucidate their microstructural features. Therefore, cumene was selected as a small-molecule model compound for structural motifs present in polystyrene (Chart 1). Adapting the methodology reported by Pyun et al.,[36] cumene was reacted with elemental sulfur in a 2:1 ratio at 230 °C with mechanical stirring for 24 h to afford the corresponding HSM, followed by reduction with $LiAlH_4$ to cleave oligo/polysulfide chains and convert them into C−SH moieties, and the resulting soluble, small-molecule species were analyzed by GC-MS (Figures S54−S59 and Scheme 2).

Chart 1. General Structure of a Chain Segment in Polystyrene and Cumene, Used as a Small-Molecule Model Compounds for Probing Reactions with Elemental Sulfur

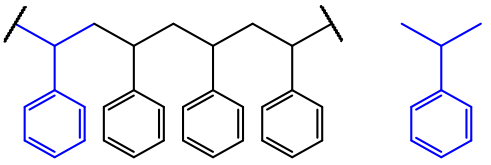

This analysis revealed a mixture of compounds containing $S-C_{(1°\ aliphatic)}$ and $S-C_{(3°\ benzylic)}$ bonds but, unexpectedly, also compounds containing $S-C_{(aryl)}$ bonds in the form of benzothiophene derivatives (Scheme 2). Compound **1** was observed by GC-MS, but given that all reactions were performed with a large excess of sulfur, it is unlikely that the material contained any olefin groups. Instead, we propose that H atom transfer from cumene generates a 3° benzylic radical that reacted with sulfur to generate an oligo/polysulfide chain attached via an $S-C_{(3°\ benzylic)}$ bond (motif **A**). Reaction with $LiAlH_4$ transformed this into a 3° benzylic thiol, but because no identifiable peaks were present, we propose that this thiol undergoes decomposition in the GC-MS experiment to generate the compound **1** observed in the depolymerization product mixture.

Indeed, when pure 2-phenyl-2-propanethiol from a commercial supplier was subjected to the same GC-MS experimental conditions as the depolymerized sample, no peaks attributable to the parent, 3° benzylic thiol were observed, and the GC-MS instead revealed two decomposition products (Figure S60−S62). The major decomposition product peak (4.8 min) and most abundant minor decomposition product peak (6.6 min) exhibited mass-fragmentation patterns consistent with α-methylstyrene and 2,3-dimethyl-2,3-diphenylbutane, respectively. All other peaks integrated to less than 2%. Notably, the α-methylstyrene decomposition product in the GC-MS of commercially available 2-phenyl-2-propanethiol was observed at the same retention time and presented the same mass-fragmentation pattern as the peak for **1** and in the GC-MS of the depolymerized cumene−sulfur product. This same depolymerized sample also revealed a minor peak at the same retention time and with the same fragmentation pattern as 2,3-dimethyl-2,3-diphenylbutane observed in the GC-MS of commercially available 2-phenyl-2-propanethiol. Presumably,

https://doi.org/10.1021/acssusresmgt.4c00085
ACS Sustainable Resour. Manage. XXXX, XXX, XXX−XXX

Scheme 2. Proposed Microstructure Motifs in the Cumene-Derived HSM and Corresponding Small-Molecule Species Generated via HSM Depolymerization Using $LiAlH_4$[a]

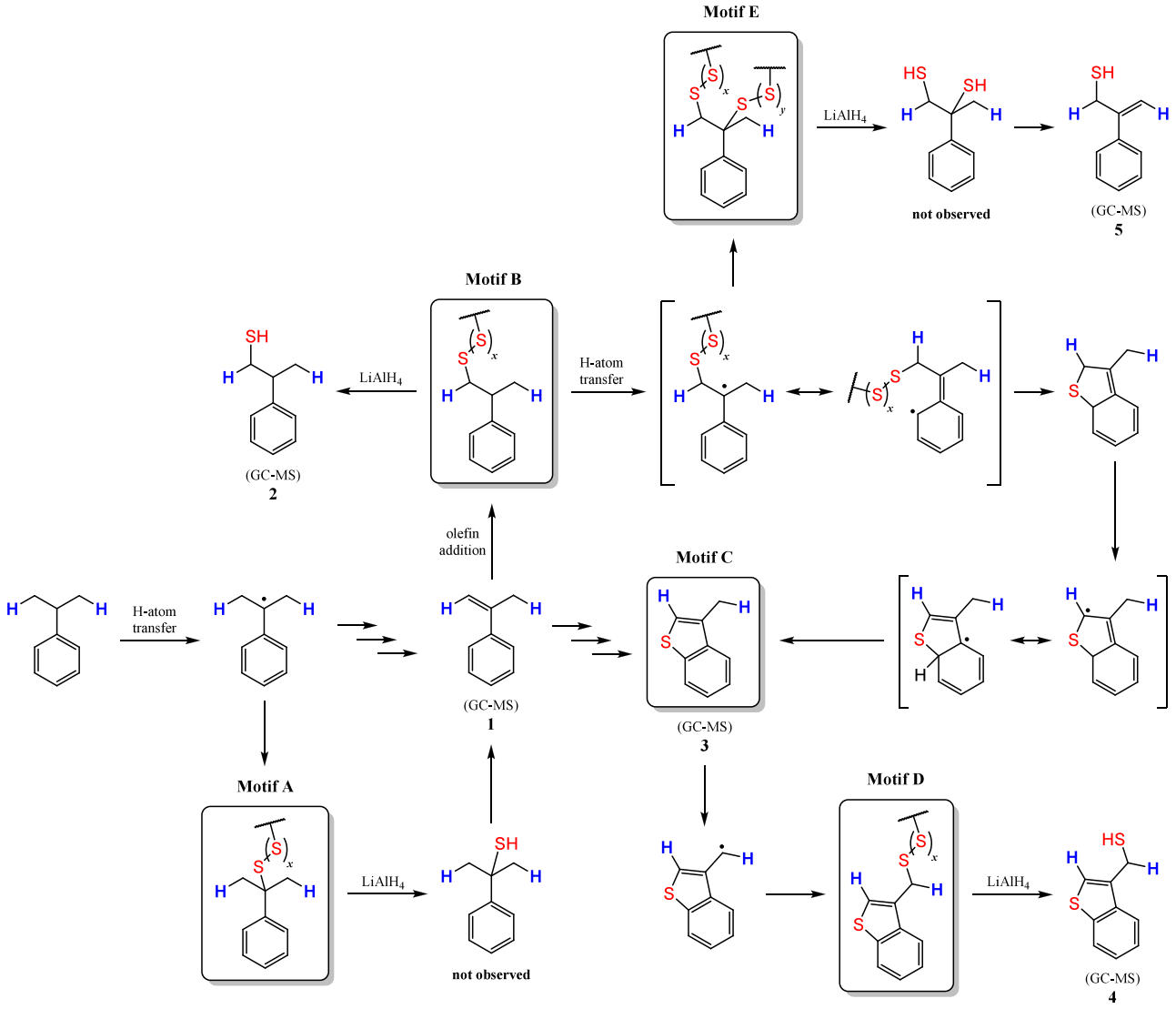

[a]One hydrogen on each of the two cumene methyl groups is explicitly represented in blue, to illustrate where the polystyrene backbone would be found in analogous PS-derived HSMs.

both α-methylstyrene and 2,3-dimethyl-2,3-diphenylbutane derive from the same 3° benzylic radical produced by C−S homolysis at that position, which readily occurs due to the stability of the 3° benzylic radical.

Compound **1** could undergo addition by oligo/polymeric sulfur radical species at the less substituted olefinic carbon to afford an $S-C_{(1^\circ\ \text{aliphatic})}$ bond, and subsequent H atom abstraction by the resulting 3° benzylic carbon radical would yield motif **B**. Reduction with $LiAlH_4$ would then convert this into compound **2**, which was observed by GC-MS. Similarly, motif **B** itself could undergo H atom transfer to generate a 3° benzylic radical, which could then undergo cyclization to form a sulfur-containing heterocycle and cleave the oligo/polysulfide chain. Subsequent H atom abstraction from this heterocycle would provide a pathway to achieve aromaticity, ultimately resulting in a benzothiophene moiety (motif **C**). Through these steps, motif **B** transforms into motif **C**, and compound **1** transforms into compound **3**. Compound **3** was observed by GC-MS, providing evidence that motif **C** was indeed present in the cumene-derived HSM.

Because the 1° carbon in motif **C** is benzylic instead of aliphatic, H atom transfer could occur at this site to generate a 1° benzylic radical, which would then react with sulfur to afford an oligo/polysulfide chain attached via an $S-C_{(1^\circ\ \text{benzylic})}$ bond (motif **D**). Depolymerization with $LiAlH_4$ would transform motif **D** into compound **4**, and the presence of GC-MS peaks consistent with **4** supported the hypothesis that the HSM precursor contained motif **D** microstructural features. Generation of carbon-centered radicals in aromatic small molecules containing thioether moieties has been previously shown to result in rearrangement and formation of fused sulfur-containing heterocycles via transformations similar to those proposed for motif **C** and motif **D**.[92]

Alternatively, the 3° benzylic radical formed via H atom transfer from motif **B** could react with sulfur to yield a second oligo/polysulfide chain, one attached via an $S-C_{(1^\circ\ \text{aliphatic})}$ bond and the other via an $S-C_{(3^\circ\ \text{benzylic})}$ bond, such that a

https://doi.org/10.1021/acssusresmgt.4c00085
ACS Sustainable Resour. Manage. XXXX, XXX, XXX−XXX

single cumene moiety would be comprised of two oligo/polysulfide chains (motif **E**). Reduction of motif **E** with $LiAlH_4$ would yield a cumene dithiol, which was not observed by GC-MS. Because compound **1** was observed following the depolymerization of motif **A**, but the 3° benzylic thiol was not, we hypothesized that a cumene dithiol would undergo a similar elimination reaction in the GC-MS experiment. In support of this hypothesis, compound **5** was observed by GC-MS, providing evidence for the presence of motif **E** in the cumene-derived HSM.

We propose that each HSM derived from polystyrene waste streams (**PSF_{90}**, **PSC_{90}**, **PSL_{90}**, **PSP_{90}**, and **PSM_{90}**) is comprised of all five of the motifs present in the cumene-derived HSM. Oligo/polysulfide chains connected to benzylic and aliphatic carbons (motif **A** and motif **B**, respectively) are present in a wide variety of previously reported HSMs, as are vicinal oligo/polysulfide chains (motif **E**).[51−53] We propose that benzothiophene moieties (motif **C** and motif **D**) form in the syntheses of **PSF_{90}**, **PSC_{90}**, **PSL_{90}**, **PSP_{90}**, and **PSM_{90}** but not the HSMs derived from styrene or triisopropylbenzene, due to the higher reaction temperatures of the former (230 vs 180 °C, respectively). Previous studies by our group on the reactions of lignin with sulfur have shown that the HSM products prepared at 230 °C are comprised of S−C bond-containing microstructural features that are absent in the corresponding HSMs prepared at 180 °C, suggesting that some bond-breaking and bond-forming transformations can occur at 230 °C but cannot at 180 °C.[93]

CONCLUSIONS

Four individual postconsumer polystyrene waste streams (flatware, foam cups, cup lids, and packaging), and a mixed-waste stream containing all four types, all underwent reaction with sulfur to afford the corresponding high-sulfur-content materials **PSF_{90}**, **PSC_{90}**, **PSL_{90}**, **PSP_{90}**, and **PSM_{90}**, respectively. Differential scanning calorimetry provided evidence that oligo/polysulfide chains anchored via S−C σ-bonds were present in each HSM, which is noteworthy because none of the PS precursors (**PSF**, **PSC**, **PSL**, **PSP**, and **PSM**) contained olefinic groups that could undergo direct addition of sulfur radicals, with these HSMs instead being produced via H atom abstraction from C(sp^3) centers by sulfur radicals.

Impressively, the compressional strengths of **PSF_{90}**, **PSC_{90}**, **PSL_{90}**, **PSP_{90}**, and **PSM_{90}** were competitive with those of C62 Brick, and their flexural strengths were competitive with those of OPC. Remarkably, these mechanical properties can be obtained from materials prepared through a process with negligible global-warming potential (−0.0058 kg CO_2 e/kg material), in contrast to the significant carbon footprint of brick and OPC production (+0.23 and +0.90 kg CO_2 e/kg material, respectively). Further environmental benefits of switching to **PSF_{90}**, **PSC_{90}**, **PSL_{90}**, **PSP_{90}**, and **PSM_{90}** include nearly 100% atom economy and zero freshwater consumption (compared to 0.6 and 1.3 L/kg for brick and OPC, respectively).

Insights into the chemical microstructures present in **PSF_{90}**, **PSC_{90}**, **PSL_{90}**, **PSP_{90}**, and **PSM_{90}** were obtained from GC-MS analyses of the products from the reaction of cumene with S_8 followed by depolymerization with $LiAlH_4$. These model compound studies suggest that these HSMs contain single oligo/polysulfide chains tethered to either a 3° benzylic or 2° aliphatic carbon, as well as vicinal oligo/polysulfide chains tethered to each carbon type, microstructural features that are ubiquitous in previously reported HSMs. Surprisingly, two distinct benzothiophene-containing compounds were also observed in the model compound studies, which suggests that **PSF_{90}**, **PSC_{90}**, **PSL_{90}**, **PSP_{90}**, and **PSM_{90}** contain similar benzothiophene moieties. To the best of our knowledge, this is the first evidence that the preparation of an HSM can also yield benzothiophene moieties, rather than only oligo/polymeric sulfur chains.

Collectively, these findings suggest that postconsumer waste polymers containing aromatic groups can yield HSMs with structural features otherwise inaccessible using other polymer classes or small molecules. The ability to form benzothiophene moieties represents an additional design parameter that could be synthetically modulated to enable access to a range of unique, new HSM properties. Furthermore, we anticipate that **PSF_{90}**, **PSC_{90}**, **PSL_{90}**, **PSP_{90}**, and **PSM_{90}** will exhibit superior durability and environmental resistance compared to C62 Brick and OPC, the results of which will be detailed in a subsequent report.

EXPERIMENTAL SECTION

Materials. Sulfur (Dugas Diesel, USA), cumene (TCI), lithium aluminum hydride ($LiAlH_4$), tetrahydrofuran (THF), ethanol, hydrochloric acid (HCl), and dichloromethane were used as received. Polystyrene was obtained directly from postconsumer disposable flatware (U.S. retailer), foam cups and lids (U.S. fast food chain), and protective polystyrene foam packaging (global shipping company). Names of commercial entities producing waste products are omitted so as not to imply endorsement or bias.

Instrumentation. Proton NMR spectra were acquired on a Bruker NEO-300 MHz at room temperature and data processed with SpinWorks 4.2.11 software. All spectra reported were calibrated to the residual solvent peak from deuterated chloroform.

Fourier transform infrared spectra were obtained using a Shimadzu IR Affinity-1S instrument with an ATR attachment operating over 400−4000 cm^{-1} at ambient temperature.

SEM and EDX were acquired on a Schottky Field Emission Scanning Electron Microscope SU5000 operating in variable pressure mode with an accelerating voltage of 15 keV.

Thermogravimetric analysis (TGA) data were recorded on a TA SDT Q600 instrument over the range 25−800 °C, with a heating rate of 10 °C min^{-1} under a flow of N_2 (20 mL min^{-1}).

DSC data were acquired (Mettler Toledo DSC 3 STARe System) over the range −60 to 140 °C with a heating rate of 10 °C·min^{-1} under a flow of N_2 (200 mL·min^{-1}). Each DSC measurement was carried out over three heat−cool cycles.

Gel permeation chromatography (GPC) was carried out on a Shimadzu GPC using a Phenogel 5u 10E4A gel column and RID 10A detector and with tetrahydrofuran as an eluent at a flow rate of 1 mL min^{-1}. A set of polystyrene standards (obtained from Polymer Source, Inc.) from 136 269 to 7 215 molecular weight was used to calibrate the GPC instrument. Data acquisitions were carried out with the Labsolutions GPC software.

The GC-MS was carried out on a Shimadzu QP2010SE system with an auto-injector (AOC-20i) equipped with the mass selective detector, having an interface temperature of 250 °C, a solvent cut time of 3.50 min, threshold of 70 eV, and mass range of 45−900 m/z. Compounds were separated using a SH-Rxi-5 MS capillary column (Restek Company, Bellefonte, USA: cross-bond 5% diphenyl/95% dimethyl polysiloxane) having dimensions 30 m (length) × 0.25 mm (diameter) × 0.25 μm (film thickness). The temperature of the injector was initialized to 280 °C. The temperature was programmed to 40 °C for 1 min and then from 40 to 320 °C at a rate of 20 °C/min and then held at 320 °C for 5 min.

UV−vis data were collected on an Agilent Technologies Cary 60 UV−vis using Simple Reads software over a range 200−800 nm with the dark sulfur content being reported at 275 nm.

https://doi.org/10.1021/acssusresmgt.4c00085
ACS Sustainable Resour. Manage. XXXX, XXX, XXX−XXX

Compressional and tensile analyses were performed on a Mark-10 ES30 test stand equipped with a M3-200 force gauge (1 kN maximum force with ±1 N resolution) with an applied force rate of 3−4 $N{\cdot}s^{-1}$. Compression cylinders were cast from silicone resin molds (Smooth-On Oomoo® 25 tin-cure) with diameters of approximately 6 mm and heights of approximately 10 mm. Samples were manually sanded to ensure uniform dimensions and measured with a digital caliper with ±0.01 mm resolution. Compressional and tensile analyses were performed in quadruplicate for each composite, and the results were averaged.

Flexural strength analysis was performed using a Mettler Toledo DMA 1 STARe System in single cantilever mode. The samples were cast from silicone resin molds (Smooth-On Oomoo® 25 tin-cure). The sample dimensions were approximately 1.5 × 10 × 18 mm. Flexural analysis was performed in triplicate, and the results were averaged. The clamping force was 1 cN·m.

Preparation of Polystyrene Flatware for Upcycling. The postconsumer disposable flatware was placed in a blender (Blendtec) and blended for several minutes, resulting in the formation of coarse aggregate.

Preparation of Polystyrene Cups for Upcycling. The postconsumer disposable flatware was placed in a blender (Blendtec) and blended for several minutes, resulting in the formation of coarse aggregate.

Preparation of Polystyrene Cup Lids for Upcycling. The postconsumer disposable cup lids were placed in a blender (Blendtec) separately and blended for several minutes, resulting in the formation of coarse aggregate.

Preparation of Protective Polystyrene Foam Packaging for Upcycling. The postconsumer disposable protective polystyrene foam packaging was placed in a blender and blended for several minutes, resulting in the formation of coarse aggregate.

General Procedure for Composite Synthesis. Elemental sulfur was introduced into a heavy walled glass pressure flask sealed with a Viton O-ring-equipped poly(tetrafluoroethylene) (PTFE) stopper with a PTFE-coated magnetic stir bar. First, sulfur was melted in an oil bath at 230 ± 2 °C. Then the indicated type of polystyrene was added to the molten sulfur in the pressure flask while stirring. The reaction mixture was stirred for an additional 24 h at 230 °C after polystyrene addition. The reaction mixture became black over the course of heating and was cooled to room temperature to isolate the black solid in each case.

CAUTION. Heating elemental sulfur with organics can result in the formation of H_2S or other gases. Such gases can be toxic, foul-smelling, and corrosive. Temperature must be carefully controlled to prevent thermal spikes, contributing to the potential for H_2S or other gas evolution. Rapid stirring shortened heating times, and very slow addition of reagents can help avoid unforeseen temperature spikes.

PSF_{90}. Prepared according to the general procedure using 4.02 g (38.6 mmol of repeat unit) of polystyrene flatware powder and 36.1 g (1126 mmol) of elemental sulfur to give 40.1 g of the title compound (100%). Elemental analysis calculated: C, 9.23; S, 90.00; H, 0.77%. Found: C, 10.46; S, 89.14; H, 0.54% (Atlantic Microlab, Inc.).

PSC_{90}. Prepared according to the general procedure using 4.01 g (38.5 mmol of repeat unit) of polystyrene cup particulate and 36.0 g (1123 mmol) of elemental sulfur to give 40.0 g of the title compound (100%). Elemental analysis calculated: C, 9.23; S, 90.00; H, 0.77%. Found: C, 10.45; S, 88.38; H, 0.60% (Atlantic Microlab, Inc.).

PSL_{90}. Prepared according to the general procedure using 4.30 g (41.3 mmol of repeat unit) of polystyrene lid particulate and 36.1 g (1126 mmol) of elemental sulfur to give 40.4 g of the title compound (100%). Elemental analysis calculated: C, 9.23; S, 90.00; H, 0.77%. Found: C, 8.89; S, 90.41; H, 0.47% (Atlantic Microlab, Inc.).

PSP_{90}. Prepared according to a modification of the general procedure as follows. Elemental sulfur (36.1 g, 1130 mmol) was first mixed with the polystyrene packaging material particulate (4.01 g, 38.5 mmol of repeat unit), and then the mixture was introduced into a heavy walled glass pressure flask sealed with a Viton O-ring-equipped PTFE stopper with a PTFE-coated magnetic stir bar. The sealed pressure flask was then placed in an oil bath at 230 ± 2 °C. The reaction mixture was then stirred for 24 h at 230 °C. After cooling to room temperature, the title compound was isolated as a black solid (40.1 g, 100%). Elemental analysis calculated: C, 9.23; S, 90.00; H, 0.77%. Found: C, 9.89; S, 89.03; H, 0.61% (Atlantic Microlab, Inc.).

Procedure for Reaction of Cumene. Elemental sulfur (1.34 g, 41.8 mmol) and cumene (0.670 g, 5.57 mmol) were introduced into a heavy walled glass pressure tube sealed with a Viton O-ring-equipped PTFE stopper with a PTFE-coated magnetic stir bar. The mixture was heated in an oil bath at 230 ± 2 °C while stirring for 24 h. After cooling to room temperature, a crude solid was recovered and used directly in reaction with $LiAlH_4$ as outlined below.

Procedure for Reaction of Cumene/Sulfur Products with $LiAlH_4$. The solid obtained from the reaction of cumene/elemental sulfur (0.101 g) was introduced into a glass vial containing a magnetic stir bar in a glovebox under an atmosphere of dry N_2(g). After that under an atmosphere of dry N_2 in a glove box, 0.083 g of $LiAlH_4$ was added into the vial with the product. The solid mixture was suspended in 10 mL of anhydrous THF, and the vial was sealed with a rubber septum. Then, the reaction was stirred for 30 min at ambient temperature under N_2(g) in the glove box. Upon completing the reaction time, the vial was taken out of the glove box and placed in an ice bath under a constant flow of N_2(g). The excess $LiAlH_4$ was quenched by very slow addition of a 10 mL sample of a mixture of THF and ethanol (9:1 v/v). Then, the mixture was poured into 25 mL of 5% (v/v) HCl solution. The organic portion was extracted with dichloromethane three times. Then volatiles were removed by rotary evaporation under reduced pressure.

■ ASSOCIATED CONTENT

Supporting Information

The Supporting Information is available free of charge at https://pubs.acs.org/doi/10.1021/acssusresmgt.4c00085.

IR and NMR spectra, GPC traces, TGA and DSC data, SEM/EDX images, and stress−strain curves for compressive, flexural, and tensile analyses (PDF)

■ AUTHOR INFORMATION

Corresponding Authors

Andrew G. Tennyson − *Department of Chemistry, Clemson University, Clemson, South Carolina 29634, United States; Department of Materials Science and Engineering, Clemson University, Clemson, South Carolina 29634, United States;* orcid.org/0000-0002-8593-2979; Email: atennys@clemson.edu

Rhett C. Smith − *Department of Chemistry, Clemson University, Clemson, South Carolina 29634, United States;* orcid.org/0000-0001-6087-8032; Email: rhett@clemson.edu

Author

Shalini K. Wijeyatunga − *Department of Chemistry, Clemson University, Clemson, South Carolina 29634, United States*

Complete contact information is available at: https://pubs.acs.org/10.1021/acssusresmgt.4c00085

Author Contributions

Conceptualization, R.C.S.; methodology, R.C.S.; formal analysis, R.C.S, S.K.W., and A.G.T.; investigation, S.K.W.; resources, R.C.S. and A.G.T.; data curation, S.K.W.; writing—original draft preparation, all authors; writing—review and editing, all authors; supervision, R.C.S. and A.G.T.; funding acquisition, R.C.S. All authors have read and agreed to the published version of the manuscript.

Funding

This research is funded by the National Science Foundation grant number CHE-2203669 awarded to R.C.S.

Notes

The authors declare no competing financial interest.

REFERENCES

(1) Advancing Sustainable Materials Management: 2018 Tables and Figures. U.S. Environmental Protection Agency: Washington, DC, 2020. https://www.epa.gov/sites/default/files/2021-01/documents/2018_tables_and_figures_dec_2020_fnl_508.pdf (accessed 2024−07−14).

(2) Yeung, C. W. S.; Teo, J. Y. Q.; Loh, X. J.; Lim, J. Y. C. Polyolefins and Polystyrene as Chemical Resources for a Sustainable Future: Challenges, Advances, and Prospects. *ACS Mater. Lett.* **2021**, *3* (12), 1660−1676.

(3) Dissanayake, P. D.; Kim, S.; Sarkar, B.; Oleszczuk, P.; Sang, M. K.; Haque, M. N.; Ahn, J. H.; Bank, M. S.; Ok, Y. S. *Environ. Res.* **2022**, *209*, 112734.

(4) Nugnes, R.; Lavorgna, M.; Orlo, E.; Russo, C.; Isidori, M. Toxic impact of polystyrene microplastic particles in freshwater organisms. *Chemosphere* **2022**, *299*, 134373.

(5) Ong, A.; Wong, Z. C.; Chin, K. L. O.; Loh, W. W.; Chua, M. H.; Ang, S. J.; Lim, J. Y. C. Enhancing the photocatalytic upcycling of polystyrene to benzoic acid: a combined computational-experimental approach for acridinium catalyst design. *Chem. Sci.* **2024**, *15* (3), 1061−1067.

(6) Xu, S.; Liu, S.; Song, W.; Zheng, N. Metal-free upcycling of plastic waste: photo-induced oxidative degradation of polystyrene in air. *Green Chem.* **2024**, *26* (3), 1363−1369.

(7) Ghalta, R.; Bal, R.; Srivastava, R. Metal-free photocatalytic transformation of waste polystyrene into valuable chemicals: advancing sustainability through circular economy. *Green Chem.* **2023**, *25* (18), 7318−7334.

(8) Nikitas, N. F.; Skolia, E.; Gkizis, P. L.; Triandafillidi, I.; Kokotos, C. G. Photochemical aerobic upcycling of polystyrene plastics to commodity chemicals using anthraquinone as the photocatalyst. *Green Chem.* **2023**, *25* (12), 4750−4759.

(9) Peng, Z.; Chen, R.; Li, H. Heterogeneous Photocatalytic Oxidative Cleavage of Polystyrene to Aromatics at Room Temperature. *ACS Sust. Chem. Eng.* **2023**, *11* (29), 10688−10697.

(10) Oh, S.; Stache, E. E. Chemical Upcycling of Commercial Polystyrene via Catalyst-Controlled Photooxidation. *J. Am. Chem. Soc.* **2022**, *144* (13), 5745−5749.

(11) Giakoumakis, N. S.; Vos, C.; Janssens, K.; Vekeman, J.; Denayer, M.; De Proft, F.; Marquez, C.; De Vos, D. Total revalorization of high impact polystyrene (HIPS): enhancing styrene recovery and upcycling of the rubber phase. *Green Chem.* **2024**, *26* (1), 340−352.

(12) Luo, X.; Zhan, J.; Mei, Q.; Zhang, S. Selective oxidative upgrade of waste polystyrene plastics by nitric acid to produce benzoic acid. *Green Chem.* **2023**, *25* (17), 6717−6727.

(13) Munyaneza, N. E.; Posada, C.; Xu, Z.; De Altin Popiolek, V.; Paddock, G.; McKee, C.; Liu, G. A Generic Platform for Upcycling Polystyrene to Aryl Ketones and Organosulfur Compounds. *Angew. Chem., Int. Ed.* **2023**, *62* (36), No. e202307042.

(14) Ong, A.; Teo, J. Y. Q.; Feng, Z.; Tan, T. T. Y.; Lim, J. Y. C. Organocatalytic Aerobic Oxidative Degradation of Polystyrene to Aromatic Acids. *ACS Sust. Chem. Eng.* **2023**, *11* (34), 12514−12522.

(15) Kumar, V.; Khan, A.; Rabnawaz, M. Efficient Depolymerization of Polystyrene with Table Salt and Oxidized Copper. *ACS Sust. Chem. Eng.* **2022**, *10* (19), 6493−6502.

(16) Chang, Y.; Blanton, S. J.; Andraos, R.; Nguyen, V. S.; Liotta, C. L.; Schork, F. J.; Sievers, C. Kinetic Phenomena in Mechanochemical Depolymerization of Poly(styrene). *ACS Sust. Chem. Eng.* **2024**, *12* (1), 178−191.

(17) Fan, S.; Zhang, Y.; Cui, L.; Xiong, Q.; Maqsood, T. Conversion of Polystyrene Plastic into Aviation Fuel through Microwave-Assisted Pyrolysis as Affected by Iron-Based Microwave Absorbents. *ACS Sust. Chem. Eng.* **2023**, *11* (3), 1054−1066.

(18) Johar, P.; Rylott, E. L.; McElroy, C. R.; Matharu, A. S.; Clark, J. H. Phytocat - a bio-derived Ni catalyst for rapid de-polymerization of polystyrene using a synergistic approach. *Green Chem.* **2021**, *23* (2), 808−814.

(19) Rabot, C.; Chen, Y.; Lin, S.-Y.; Miller, B.; Chiang, Y.-M.; Oakley, C. E.; Oakley, B. R.; Wang, C. C. C.; Williams, T. J. Polystyrene Upcycling into Fungal Natural Products and a Biocontrol Agent. *J. Am. Chem. Soc.* **2023**, *145* (9), 5222−5230.

(20) Yang, W.; Li, H.; Wu, Q.; Ren, Y.; Shi, D.; Zhao, Y.; Jiao, Q. Functionalized Core-Shell Polystyrene Sphere-Supported Alkaline Imidazolium Ionic Liquid: An Efficient and Recyclable Catalyst for Knoevenagel Condensation. *ACS Sust. Chem. Eng.* **2020**, *8* (49), 18126−18137.

(21) Li, C.; Cai, X.; Tian, Z.; Ji, X.; Wang, Q. Biobased Microspheres with Nanoshell/Micron-Core Structure via Recycled Polystyrene toward Electrophoretic Imaging. *ACS Sust. Chem. Eng.* **2023**, *11* (25), 9288−9294.

(22) Liu, A.; Mollart, C.; Trewin, A.; Fan, X.; Lau, C. H. Photo-Modulating CO2 Uptake of Hypercrosslinked Polymers Upcycled from Polystyrene Waste. *ChemSusChem* **2023**, *16* (10), No. e202300019.

(23) Mineral commodity summaries 2024. U.S. Geological Survey: Reston, VA, 2024. https://pubs.usgs.gov/periodicals/mcs2024/mcs2024.pdf (accessed 2024−07−14).

(24) Rappold, T. A.; Lackner, K. S. Large scale disposal of waste sulfur: From sulfide fuels to sulfate sequestration. *Energy* **2010**, *35* (3), 1368−1380.

(25) Crescenzi, F.; Crisari, A.; D'Angel, E.; Nardella, A. Control of Acidity Development on Solid Sulfur Due to Bacterial Action. *Environ. Sci. Technol.* **2006**, *40* (21), 6782−6786.

(26) Zhang, X.; Tang, Y.; Qu, S.; Da, J.; Hao, Z. H2S-Selective Catalytic Oxidation: Catalysts and Processes. *ACS Catal.* **2015**, *5* (2), 1053−1067.

(27) Demirbas, A.; Alidrisi, H.; Balubaid, M. A. API Gravity, Sulfur Content, and Desulfurization of Crude Oil. *Petroleum Science and Technology* **2015**, *33* (1), 93−101.

(28) Wolfs, J.; Ribca, I.; Meier, M. A. R.; Johansson, M. Polythionourethane Thermoset Synthesis via Activation of Elemental Sulfur in an Efficient Multicomponent Reaction Approach. *ACS Sust. Chem. Eng.* **2023**, *11* (9), 3952−3962.

(29) Conen, P.; Nickisch, R.; Meier, M. A. R. Synthesis of highly substituted alkenes by sulfur-mediated olefination of N-tosylhydrazones. *Commun. Chem.* **2023**, *6* (1), 255.

(30) Nickisch, R.; Conen, P.; Gabrielsen, S. M.; Meier, M. A. R. A more sustainable isothiocyanate synthesis by amine catalyzed sulfurization of isocyanides with elemental sulfur. *RSC Adv.* **2021**, *11* (5), 3134−3142.

(31) Zhang, Y.; Glass, R. S.; Char, K.; Pyun, J. Recent advances in the polymerization of elemental sulphur, inverse vulcanization and methods to obtain functional Chalcogenide Hybrid Inorganic/Organic Polymers (CHIPs). *Polym. Chem.* **2019**, *10* (30), 4078−4105.

(32) Chalker, J. M.; Worthington, M. J. H.; Lundquist, N. A.; Esdaile, L. J. Synthesis and Applications of Polymers Made by Inverse Vulcanization. *Top. Curr. Chem.* **2019**, *377* (3), 1−27.

(33) Abbasi, A.; Nasef, M. M.; Yahya, W. Z. N. Sulfur-based polymers by inverse vulcanization: a novel path to foster green chemistry. *Green Mater.* **2020**, *8* (4), 172−180.

(34) Wagenfeld, J.-G.; Al-Ali, K.; Almheiri, S.; Slavens, A. F.; Calvet, N. Sustainable applications utilizing sulfur, a by-product from oil and gas industry: A state-of-the-art review. *Waste Management* **2019**, *95*, 78−89.

(35) Abbasi, A.; Nasef, M. M.; Yahya, W. Z. N. Copolymerization of vegetable oils and bio-based monomers with elemental sulfur: A new promising route for bio-based polymers. *Sust. Chem. Pharm.* **2019**, *13*, 100158.

https://doi.org/10.1021/acssusresmgt.4c00085
ACS Sustainable Resour. Manage. XXXX, XXX, XXX−XXX

(36) Bao, J.; Martin, K. P.; Cho, E.; Kang, K.-S.; Glass, R. S.; Coropceanu, V.; Bredas, J.-L.; Parker, W. O. N., Jr; Njardarson, J. T.; Pyun, J. On the Mechanism of the Inverse Vulcanization of Elemental Sulfur: Structural Characterization of Poly(sulfur-random-(1,3-diisopropenylbenzene)). *J. Am. Chem. Soc.* **2023**, *145* (22), 12386−12397.
(37) Chung, W. J.; Griebel, J. J.; Kim, E. T.; Yoon, H.; Simmonds, A. G.; Ji, H. J.; Dirlam, P. T.; Glass, R. S.; Wie, J. J.; Nguyen, N. A.; et al. The use of elemental sulfur as an alternative feedstock for polymeric materials. *Nat. Chem.* **2013**, *5* (6), 518−524.
(38) Mueller, F. G.; Lisboa, L. S.; Chalker, J. M. Inverse Vulcanized Polymers for Sustainable Metal Remediation. *Adv. Sustainable Syst.* **2023**, *7* (5), 2300010.
(39) Mann, M.; Pauling, P. J.; Tonkin, S. J.; Campbell, J. A.; Chalker, J. M. Chemically Activated S-S Metathesis for Adhesive-Free Bonding of Polysulfide Surfaces. *Macromolecular Chemistry and Physics* **2022**, *223* (13), 2100333.
(40) Gupta, A.; Worthington, M. J. H.; Patel, H. D.; Johnston, M. R.; Puri, M.; Chalker, J. M. Reaction of sulfur and sustainable algae oil for polymer synthesis and enrichment of saturated triglycerides. *ACS Sust. Chem. Eng.* **2022**, *10* (28), 9022−9028.
(41) Tikoalu, A. D.; Lundquist, N. A.; Chalker, J. M. Mercury Sorbents Made By Inverse Vulcanization of Sustainable Triglycerides: The Plant Oil Structure Influences the Rate of Mercury Removal from Water. *Adv. Sustainable Syst.* **2020**, *4* (3), 1900111.
(42) Worthington, M. J. H.; Kucera, R. L.; Chalker, J. M. Green chemistry and polymers made from sulfur. *Green Chem.* **2017**, *19* (12), 2748−2761.
(43) Yan, P.; Zhao, W.; McBride, F.; Cai, D.; Dale, J.; Hanna, V.; Hasell, T. Mechanochemical synthesis of inverse vulcanized polymers. *Nat. Commun.* **2022**, *13* (1), 4824.
(44) Jia, J.; Liu, J.; Wang, Z.-Q.; Liu, T.; Yan, P.; Gong, X.-Q.; Zhao, C.; Chen, L.; Miao, C.; Zhao, W.; et al. Photoinduced inverse vulcanization. *Nat. Chem.* **2022**, *14* (11), 1249−1257.
(45) Petcher, S.; Zhang, B.; Hasell, T. Mesoporous knitted inverse vulcanized polymers. *Chem. Commun. (Cambridge, U. K.)* **2021**, *57* (41), 5059−5062.
(46) Zhang, B.; Gao, H.; Yan, P.; Petcher, S.; Hasell, T. Inverse vulcanization below the melting point of sulfur. *Materials Chemistry Frontiers* **2020**, *4* (2), 669−675.
(47) Wu, X.; Smith, J. A.; Petcher, S.; Zhang, B.; Parker, D. J.; Griffin, J. M.; Hasell, T. Catalytic inverse vulcanization. *Nat. Commun.* **2019**, *10* (1), 10035−10044.
(48) Eder, M. L.; Call, C. B.; Jenkins, C. L. Utilizing Reclaimed Petroleum Waste to Synthesize Water-Soluble Polysulfides for Selective Heavy Metal Binding and Detection. *ACS Appl. Polym. Mater.* **2022**, *4* (2), 1110−1116.
(49) Orme, K.; Fistrovich, A. H.; Jenkins, C. L. Tailoring Polysulfide Properties through Variations of Inverse Vulcanization. *Macromolecules* **2020**, *53* (21), 9353−9361.
(50) Westerman, C. R.; Jenkins, C. L. Dynamic Sulfur Bonds Initiate Polymerization of Vinyl and Allyl Ethers at Mild Temperatures. *Macromolecules* **2018**, *51* (18), 7233−7238.
(51) Zhang, Y.; Griebel, J. J.; Dirlam, P. T.; Nguyen, N. A.; Glass, R. S.; MacKay, M. E.; Char, K.; Pyun, J. Inverse vulcanization of elemental sulfur and styrene for polymeric cathodes in Li-S batteries. *J. Polym. Sci., Part A: Polym. Chem.* **2017**, *55* (1), 107−116.
(52) Pyun, J.; Carrozza, C. F.; Silvano, S.; Boggioni, L.; Losio, S.; de Angelis, A. R.; O'Neil Parker, W., Jr Nuclear magnetic resonance structural characterization of sulfur-derived copolymers from inverse vulcanization. Part 1: Styrene. *Journal of Polymer Science (Hoboken, NJ, United States)* **2022**, *60* (24), 3471−3477.
(53) Lai, Y.-S.; Liu, Y.-L. Reaction between 1,3,5-Triisopropylbenzene and Elemental Sulfur Extending the Scope of Reagents in Inverse Vulcanization. *Macromol. Rapid Commun.* **2023**, *44* (8), 2300014.
(54) Cassidy, K.; Elyashiv-Barad, S. US FDA's revised consumption factor for polystyrene used in food-contact applications. *Food Addit. Contam.* **2007**, *24* (9), 1026−1031.
(55) Brun, N.; Bourson, P.; Margueron, S. Quantification of rubber in high impact polystyrene by Raman spectroscopy. Comparison of a band fitting method and chemometrics. *Vib. Spectrosc.* **2013**, *67*, 55−60.
(56) Lacoste, J.; Delor, F.; Pilichowski, J. F.; Singh, R. P.; Prasad, A. V.; Sivaram, S. Polybutadiene Content and Microstructure in HighImpact Polystyrene. *J. Appl. Polym. Sci.* **1996**, *59* (6), 953−959.
(57) Dale, J. J.; Stanley, J.; Dop, R. A.; Chronowska-Bojczuk, G.; Fielding, A. J.; Neill, D. R.; Hasell, T. Exploring Inverse Vulcanisation Mechanisms from the Perspective of Dark Sulfur. *European Polymer Journal* **2023**, *195*, 112198.
(58) Dale, J. J.; Petcher, S.; Hasell, T. Dark Sulfur: Quantifying Unpolymerized Sulfur in Inverse Vulcanized Polymers. *ACS Appl. Polym. Mater.* **2022**, *4* (5), 3169−3173.
(59) Wijeyatunga, S. K.; Derr, K. M.; Maladeniya, C. P.; Sauceda-Oloño, P. Y.; Tennyson, A. G.; Smith, R. C. Upcycling waste PMMA to durable composites via a transesterification-inverse vulcanization process. *Journal of Polymer Science* **2023**, *62* (3), 554−563.
(60) Derr, K. M.; Lopez, C. V.; Maladeniya, C. P.; Tennyson, A. G.; Smith, R. C. Transesterification-vulcanization route to durable composites from post-consumer poly(ethylene terephthalate), terpenoids, and industrial waste sulfur. *Journal of Polymer Science* **2023**, *61*, 3075−3086.
(61) Derr, K. M.; Smith, R. C. One-Pot Method for Upcycling Polycarbonate Waste to Yield High-Strength, BPA-Free Composites. *Journal of Polymer Science* **2024**, *62*, 1115−1122.
(62) Dale, J. J.; Stanley, J.; Dop, R. A.; Chronowska-Bojczuk, G.; Fielding, A. J.; Neill, D. R.; Hasell, T. Exploring Inverse Vulcanisation Mechanisms from the Perspective of Dark Sulfur. *European Polymer Journal* **2023**, *195*, 112198.
(63) Hoefling, A.; Lee, Y. J.; Theato, P. Sulfur-Based Polymer Composites from Vegetable Oils and Elemental Sulfur: A Sustainable Active Material for Li-S Batteries. *Macromol. Chem. Phys.* **2017**, *218* (1), 1600303.
(64) Wreczycki, J.; Bielinski, D. M.; Anyszka, R. Sulfur/organic copolymers as curing agents for rubber. *Polymers (Basel, Switzerland)* **2018**, *10* (8), 870.
(65) Lopez, C. V.; Karunarathna, M. S.; Lauer, M. K.; Maladeniya, C. P.; Thiounn, T.; Ackley, E. D.; Smith, R. C. High Strength, Acid-Resistant Composites from Canola, Sunflower, or Linseed Oils: Influence of Triglyceride Unsaturation on Material Properties. *J. Poly. Sci.* **2020**, *58*, 2259−2266.
(66) Maladeniya, C. P.; Karunarathna, M. S.; Lauer, M. K.; Lopez, C. V.; Thiounn, T.; Smith, R. C. A Role for Terpenoid Cyclization in the Atom Economical Polymerization of Terpenoids with Sulfur to Yield Durable Composites. *Materials Advances* **2020**, *1*, 1665−1674.
(67) Bandzierz, K.; Reuvekamp, L.; Dryzek, J.; Dierkes, W.; Blume, A.; Bielinski, D. Influence of network structure on glass transition temperature of elastomers. *Materials* **2016**, *9* (7), 607−607.
(68) Zaper, A. M.; Koenig, J. L. Solid-state carbon-13 NMR studies of vulcanized elastomers. 4. Sulfur-vulcanized polybutadiene. *Makromol. Chem.* **1988**, *189* (6), 1239−1251.
(69) Thiounn, T.; Karunarathna, M. S.; Lauer, M. K.; Tennyson, A. G.; Smith, R. C. Detoxification of bisphenol A via sulfur-mediated carbon-carbon σ-bond scission. *RSC Sustainability* **2023**, *1* (3), 535−542.
(70) Thiounn, T.; Lauer, M. K.; Karunarathna, M. S.; Tennyson, A. G.; Smith, R. C. Copolymerization of a Bisphenol a Derivative and Elemental Sulfur by the RASP Process. *Sus. Chem.* **2020**, *1*, 183−197.
(71) Maladeniya, C. P.; Tennyson, A. G.; Smith, R. C. Single-stage chemical recycling of plastic waste to yield durable composites via a tandem transesterification-thiocracking process. *Journal of Polymer Science* **2023**, *61* (9), 787−793.
(72) Lopez, C. V.; Smith, R. C. Composites produced from Waste Plastic with Agricultural and Energy Sector By-Products. *J. Appl. Polym. Sci.* **2024**, *141*, No. e54828.
(73) Lopez, C. V.; Smith, R. C. Chemical Recycling of Poly(ethylene terephthalate) via Sequential Glycolysis, Oleoyl Chloride Esterifica-

https://doi.org/10.1021/acssusresmgt.4c00085
ACS Sustainable Resour. Manage. XXXX, XXX, XXX−XXX

tion and Vulcanization to yield Durable Composites. *Materials Advances* **2023**, *4*, 2785−2793.
(74) Yan, P.; Zhao, W.; Tonkin, S. J.; Chalker, J. M.; Schiller, T. L.; Hasell, T. Stretchable and Durable Inverse Vulcanized Polymers with Chemical and Thermal Recycling. *Chem. Mater.* **2022**, *34* (3), 1167−1178.
(75) Smith, J. A.; Green, S. J.; Petcher, S.; Parker, D. J.; Zhang, B.; Worthington, M. J. H.; Wu, X.; Kelly, C. A.; Baker, T.; Gibson, C. T.; et al. Crosslinker Copolymerization for Property Control in Inverse Vulcanization. *Chem.—Eur. J.* **2019**, *25* (44), 10433−10440.
(76) Dale, J. J.; Hanna, V.; Hasell, T. Manipulating Inverse Vulcanization Comonomers to Generate High-Tensile-Strain Polymers. *ACS Appl. Polym. Mater.* **2023**, *5* (9), 6761−6765.
(77) Stojcevski, F.; Stanfield, M. K.; Hayne, D. J.; Mann, M.; Lundquist, N. A.; Chalker, J. M.; Henderson, L. C. Inverse Vulcanisation of canola oil as a route to recyclable chopped carbon fibre composites. *Sustainable Materials and Technologies* **2022**, *32*, No. e00400.
(78) Thiounn, T.; Lauer, M. K.; Bedford, M. S.; Smith, R. C.; Tennyson, A. G. Thermally-healable network solids of sulfur-crosslinked poly(4-allyloxystyrene). *RSC Adv.* **2018**, *8* (68), 39074−39082.
(79) Derr, K. M.; Smith, R. C. One-Pot Method for Upcycling Polycarbonate Waste to Yield High-Strength, BPA-Free Composites. *J. Polymer Sci.* **2024**, *62*, 1115−1122.
(80) Derr, K. M.; Lopez, C. V.; Maladeniya, C. P.; Tennyson, A. G.; Smith, R. C. Transesterification-vulcanization route to durable composites from post-consumer poly(ethylene terephthalate), terpenoids, and industrial waste sulfur. *Journal of Polymer Science* **2023**, *61*, 3075.
(81) Sheldon, R. A. The E Factor: fifteen years on. *Green Chem.* **2007**, *9* (12), 1273−1283.
(82) Brogaard, L. K.; Damgaard, A.; Jensen, M. B.; Barlaz, M.; Christensen, T. H. Evaluation of life cycle inventory data for recycling systems. *Resources, Conservation and Recycling* **2014**, *87*, 30−45.
(83) Passarini, F.; Ciacci, L.; Santini, A.; Vassura, I.; Morselli, L. Auto shredder residue LCA: implications of ASR composition evolution. *Journal of Cleaner Production* **2012**, *23* (1), 28−36.
(84) Arena, U.; Ardolino, F. Technical and environmental performances of alternative treatments for challenging plastics waste. *Resources, Conservation and Recycling* **2022**, *183*, 106379.
(85) Jeswani, H.; Krüger, C.; Russ, M.; Horlacher, M.; Antony, F.; Hann, S.; Azapagic, A. Life cycle environmental impacts of chemical recycling via pyrolysis of mixed plastic waste in comparison with mechanical recycling and energy recovery. *Science of the Total Environment* **2021**, *769*, 144483.
(86) Wüstenberg, D.; Kasper, J. Required energy and structural breakdown at the process of dynamic cutting—comminution of polypropylene and aluminium. *Int. J. Miner. Process.* **2004**, *74*, S417−S424.
(87) Schubert, G.; Bernotat, S. Comminution of non-brittle materials. *Int. J. Miner. Process.* **2004**, *74*, S19−S30.
(88) Peukert, W. Material properties in fine grinding. *Int. J. Miner. Process.* **2004**, *74*, S3−S17.
(89) Lewis, G. N.; Randall, M. THE HEAT CONTENT OF THE VARIOUS FORMS OF SULFUR. *J. Am. Chem. Soc.* **1911**, *33* (4), 476−488.
(90) Scrivener, K. L.; John, V. M.; Gartner, E. M. Eco-efficient cements: Potential economically viable solutions for a low-CO2 cement-based materials industry. *Cement and Concrete Research* **2018**, *114*, 2−26.
(91) Scrivener, K. L.; Fullmann, T.; Gallucci, E.; Walenta, G.; Bermejo, E. Quantitative study of Portland cement hydration by X-ray diffraction/Rietveld analysis and independent methods. *Cement and Concrete Research* **2004**, *34* (9), 1541−1547.
(92) Capella, L.; Montevecchi, P. C.; Nanni, D. Tin Radical Addition to Alkynyl Sulfides: Reactivity of the Intermediate Thioalkyl-Substituted ß-(Tributylstannyl)vinyl Radicals. *Journal of Organic Chemistry* **1994**, *59* (12), 3368−3374.
(93) Kapuge Dona, N. L.; Maladeniya, C. P.; Smith, R. C. Reactivity of Biomass-Derived Olefins with Elemental Sulfur: Mechanistic Insight. *European Journal of Organic Chemistry* **2024**, *27* (14), No. e202301269.

https://doi.org/10.1021/acssusresmgt.4c00085
ACS Sustainable Resour. Manage. XXXX, XXX, XXX−XXX